Width variations of hydrodynamically focused streams in low to moderate Reynolds number
Proceedings of European Congress of Chemical Engineering (ECCE-6)
Copenhagen, 16-20 September 2007

Width variations of hydrodynamically focused streams in low to moderate Reynolds number

Piotr Michal Domagalski[a], Marek Dziubinski[a], Pawel Budzynski[a], Michal Marek Mielnik[b], Lars Roar Saetran[c]

[a]*Faculty of Process and Environmental Engineering, Technical University of Lodz, Wolczanska 213, 90-924 Lodz, Poland*
[b]*SINTEF ICT, Microsystems and Nanotechnology, P.O. Box 124 Blindern, N-0314 Oslo, Norway*
[c]*Department of Process and Energy Engineering, Norwegian University of Science and Technology, Kolbjorn Hejes v 1B, 7491 Trondheim, Norway*

Abstract

Hydrodynamic focusing is a widely used technique in the microfluidic world. Our research shows a new, complicated three-dimensional aspect of this phenomenon indicating novel, promising possibilities of future applications and development

Keywords: microfluidics, hydrodynamic focusing

1. Introduction

In the last decade one of the quickest developing trends in chemical engineering area is microfluidics, covering the issues of heat, mass and momentum transfer in microscale. This corresponds directly to intensive research of nano- and microscale technology, as in such scales the system behavior shows significant deviations, compared to macroscale. That is mainly due to drastically different surface to volume ratio and minor role of buoyancy and inertia forces compared to surface forces like surface tension and adhesion.
One of the phenomena involved in a growing number of applications within the microfluidics area is hydrodynamic focusing being a technique used to introduce the sample streak into the capillary axis by reshaping and squeezing the initial stream by side inert streams.
In the case of four rectangular channels intersection geometry it can be described as squeezing the main stream in intersection by two side streams, reshaping it downstream into a thin, sheathed film. As can be seen in Fig 1, the stream of interest Q_C is focused and sheathed downstream by streams Q_B and Q_A

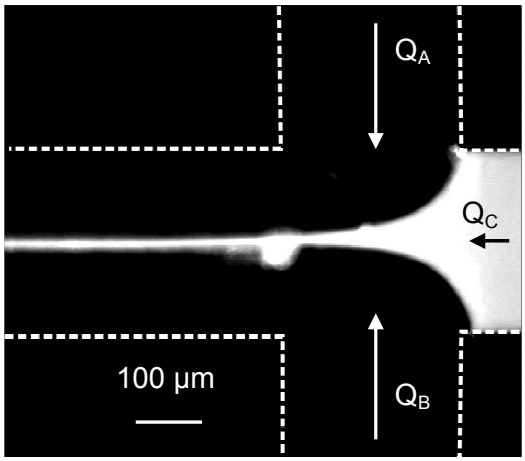

Fig 1. Fluorescent microscopy image of hydrodynamic focusing

It is a well know phenomenon in the area of fluid mechanics thanks to Osborne Reynolds, who first used it for flow visualization in his breakthrough experiment [Reynolds 1883]. Due to specific features it has been successfully involved in several microfluidic applications ranging from ultra fast mixers and reactors via flow addressing in Lab-on-a-chip applications and cytometry, two-phase systems generators, rheometry, flow visualization to microfabrication (see [Dziubinski 2007] for a detailed review).

Although the number of applications grows in number, its basic issues remain uncovered. A closer look into hydrodynamics of such a system reveals its complexity. The initial CFD investigation in 100×100 μm^2 (w×h) channels shows unexpected significant width variations across focused stream span. The postprocessed results of CFD simulations* are visible in Fig 2. The boundary conditions were set as 43,2 µl/s of total flow rate, which corresponds to mean velocity of 7,2 cm/s in outlet channel and Reynolds number of 6,42.

The observed deformations of focused streak can play an important role in existing applications, as up to day the phenomenon of hydrodynamic focusing has been treated as two dimensional in the literature. At the same time, the discovered focused streak behavior is indicating new directions of development of the hydrodynamic focusing technique.

The cross-sectional shape of the focused streak can have an important impact in case of applications taking the advantage of sub-micrometer precision. Such a level of control may be needed in many novel applications involving controlling the streak position across an outlet channel (Kenis 1999, Takayama 2003, Kam 2003). Those examples, relying on wall –focused stream (or wall anchored object – focused stream) interaction show the importance of discovered 3D aspect.

---

* ANSYS CFX 10 software, unstructured grid, algebraic, multigrid solver, and second order upwind scheme.

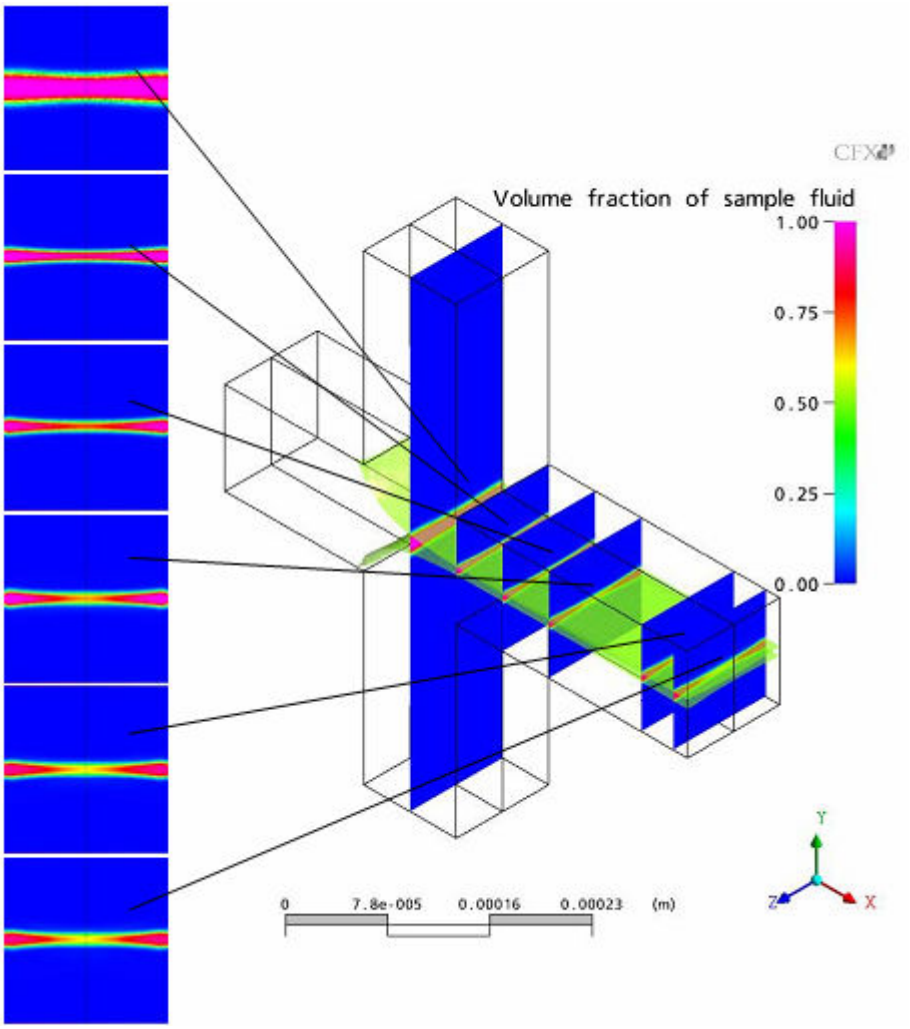

Fig 2. CFD of hydrodynamic focusing [Lunde 2005]. Visible extracted cross-sections showing the width deformations of focused streak

2. Experimental setup

To investigate the three-dimensional aspect of hydrodynamic focusing, Confocal Laser Scanning Microscopy (CLSM) was applied. The CLSM is a microscopy technique capable of delivering high quality images of thick specimens by blocking the out-of-focus light before reaching the detector. This is done by a pinhole sitting conjugated to the focal plane. The excellently sharp images taken from sequenced, densely spaced planes can be assembled into a complete 3D projection rendering this technique highly recommended for complicated 3D flow visualization in microscale [Park 2004].
In our case, we used a Carl Zeiss CSM 510 microscope with 8 bit CCD array, Plan-Neofluar 20x/0.5 and C-Apochromat 10x/0.45W objectives with HeNe 543 nm and Argon 488 nm laser from LASOS Lasertechnik as a light source.

Channels for the experiment were done by micromilling in polymethyl metacrylate (PMMA) and thermally bonded with pre-drilled cover slip. The cross sections of investigated channels were 260x200 μm^2 (w×h). The flow was driven by a PHD 2000 syringe pump (Harvard Apparatus). For the flow-media we used deionised water and fluorescent dye (Alexa Fluor 546 by Molecular Probes and FITC-Dextran by Sigma-Aldrich).

3. Results and discussion

The detailed flow pattern analysis revealed three, dependent on overall flow velocity, possible 'regimes' of focused streak shape: the barrel like shape, characterized by decrease of width towards the top and bottom walls (Fig 3a), the flat – uniform shape (Fig 3b), and the hour-glass like shape, where the focused stream has double-concaved shape (Fig 3c).

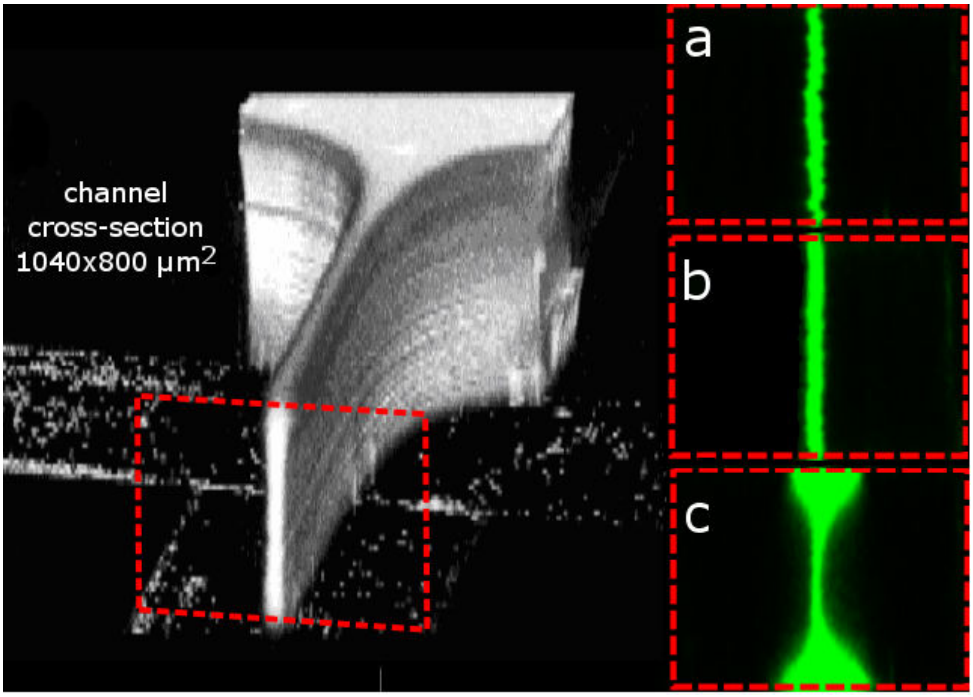

Fig. 3. The 3D projection of confocal microscopy image of hydrodynamic focusing with corresponding cross-sections; velocities in the outlet channel: a) 1,66 cm/s; b) 3,32 cm/s; c) 6,65 cm/s and corresponding Reynolds number 3,23 6,46 and 12,92.

The focused stream remained flat within the range of total flow rate from Q = 0,00133 ml/s (corresponding to mean velocity in the outlet channel v = 2,53 cm/s, Reynolds number Re = 5,17) to Q = 0,002 ml/s (corresponding to mean velocity in the outlet channel v = 3,84 cm/s, Reynolds number Re = 7,75). Above this range, the streak cross-section had double concaved shape, whereas the barrel-like shape occurred for flow rates beneath this range. The limits for investigated velocities (and Reynolds numbers) were set by armature limitation on the upper side, and pump precision on the lower side, and were about Re = 1,5 and Re=20. A change from water into 1 %

w/w glucose solution was done to check the focused stream morphology in creeping flow (down to Re = 0,15).
To explain the described behavior, we try to look closely into hydrodynamics of such a system. Several effects which can influence the flow pattern can be isolated and discussed.
First of all the centrifugal effects. If we look at Fig 4. showing the flow field in geometry midsection* and isolate stream-lines originating from a side stream we notice that the pattern resemble the flow in curved duct. That means that we should expect the swirling secondary flow pattern due to imbalance of centripetal forces. That pattern is similar to Dean flow and its presence, in case of hydrofocusing, has been proven by CFD.

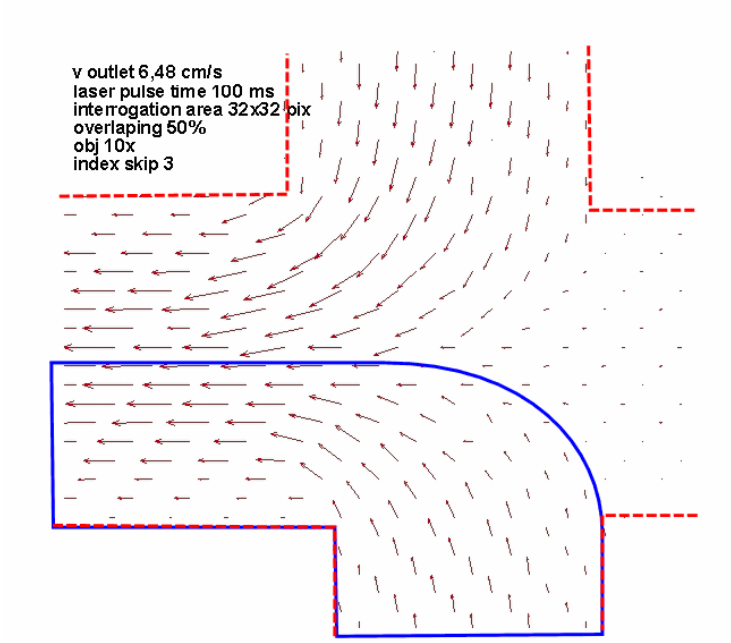

Fig 4. Processed μ-PIV image of hydrodynamic focusing (mid-plane of 260×200 μm^2 channel intersection)

The visible difference between curved duct and hydrofocusing geometry is the existence of sharp bend resulting in early (in lower Reynolds number than in case of curved duct) flow separation. The growing with velocity, separated region of flow will influence the flow pattern. In low Reynolds number, on the other hand, the separated region will vanish. Domination of viscosity, however, and the fluid flow around sharp corner in these conditions will result in different flow pattern [Moffat 1964].

* the flow field was obtained by μPIV technique (Olympus BX51 with 10x/0.3 PlanFluor obj, Nd-YAG laser from Continuum and Dantec Flow Manager / TecPlot Software). See [Mielnik 2005] for setup details

The “forehead collision” of side streams, which takes place in hydrodynamic focusing has an effect on the flow z velocity component (according to coordinates from Fig. 2) as well. Both of side streams have parabolic momentum distribution due to their development as they enter the intersection. The momentum being at a maximum at the channel centre will result in a mass displacement within the focused sample streak towards the edges. The two parabolic force fields are equal in magnitude and directed in opposite directions allowing to cancel each other out along a vertical line in the centre of the channel, creating a symmetric concave stream.

The diffusion has its contribution in creation of such shaped stream as well. In flows characterized by low Reynolds number the rate of transport due to diffusion can be at the same order of magnitude as the rate of convective transport. As the diffusion of a molecule is diversely proportional to its diameter (and via diameter to its molecular weight) the participation of diffusion in global effect of sample streak deformation can be easily visualized in lab environment by using the dyes of different molecular weight (MW).

Primary used Alexa Fluor 546 dye (by Molecular Probes, MW 1079,39) allowed us to observe the diffusion effect caused the streak widening and blurring the dye-inert fluid boundaries. The change to FITC bounded with dextran (by Sigma-Aldrich) excluded the diffusion effect due to big molecular weight of dye molecule (MW 250 000). The comparison between those dyes allows us to see the participation of the diffusion effect in overall flow pattern.

The diffusion in described conditions has other important aspect due to a parabolic velocity distribution. Fluid elements will have different velocity depending on a position across the channel cross section, which together with the uniform, concentration dependant diffusion speed, means that diffusion to convection ratio differs locally. Due to the lower near wall velocity, at a given distance from the cross section the top and bottom parts of streak are diffused, what corresponds directly to widening. This phenomenon has been, in case of T-sensor, analyzed and visualized by [Kamholtz 2001].

Considering more general case we shall comment on surface effects. When operating the media of different physical characteristics we could expect the surface tension will influence the flow pattern. In case of different surface tension of inert streams and focused streak the streak cross-section will loose the rectangular cross-section depending on focused stream wetting angle (in contact with wall material). What more, the double concave cross-section will act stabilizing the central position of focused stream.

To illustrate the importance of described effect we should compare lab results with the simple 2D model neglecting the velocity distribution. Such a model can be described by equation 1.

$$\frac{Q_{DYE}}{\sum Q_{TOT}} = \frac{S}{S_D} \qquad \frac{Q_{DYE}}{\sum Q_{TOT}} = \frac{w_D}{w} \tag{1}$$

Where: Q_{DYE} is the flow rate of dye stream, Q_{TOT} is the sum of flowrates coming into the intersection, S is the channel cross-sectional area, S_D is the focused streak cross-sectional area, w is the channel width, and w_D is the focused streak width.

According to such a model, the ratio of streak width to channel width equals the ratio of dye stream flow ratio to total flow rate (sum of side streams and dye stream). As we can see in Fig 5 that is not the case. In this figure, the presented model is compared with observed focused streak width. The quantitative comparison is possible as the lab measurements were taken in conditions ensuring constant streak width (that is the case for Reynolds number between 5 to 8 in case of 260×200 μm^2 channel and water as working medium). The visible in Fig 5 dissonance shows clearly that 3D velocity distribution has to be included in hydrodynamic focusing systems design to avoid serious misspecification even in case of constant width. The situation complicates dramatically in case of streak deformations as described above, as these deformations change the flow pattern, greatly increasing the gap between the predictions and the experimentally observed flow pattern.

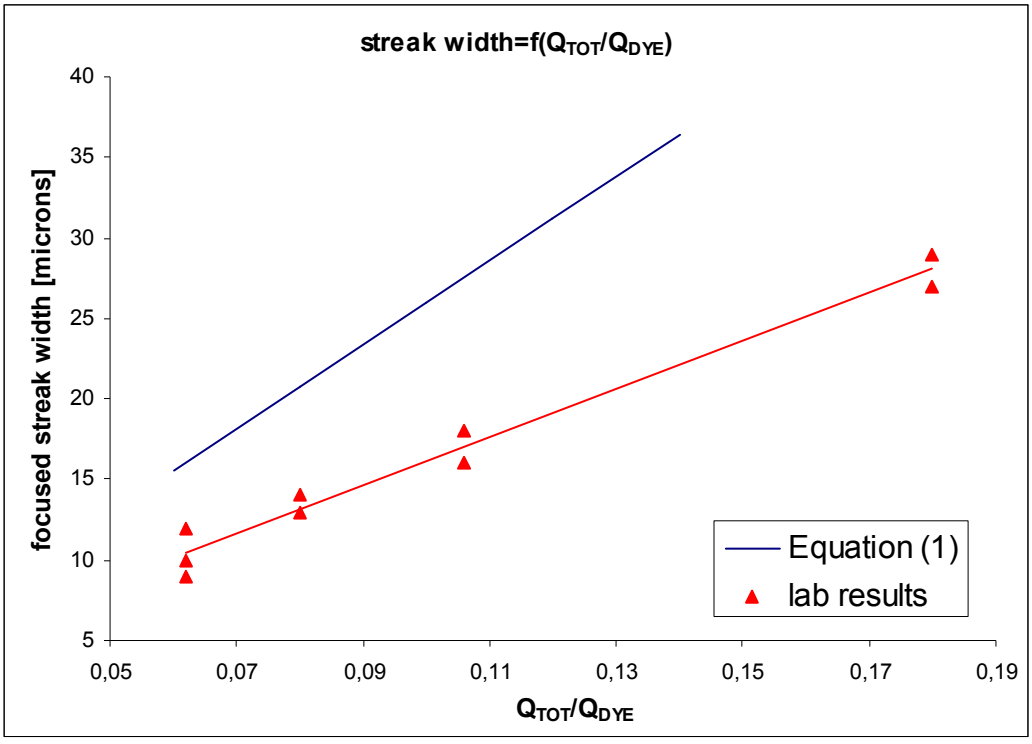

Fig 5. Comparison of focused streak width calculated from simplified 2D model (eq. 1) and lab results

4. Summary

Described effects driving to changes in a 3D structure of focused stream indicate the precautions in designing the hydrofocusing systems. The whole system behavior is dependant on synergy of described effects, which are independently changing with velocity. The possible shapes and stream deformations can be explained by changes in mechanisms taking the lead and major contribution in influence of flow pattern. The complexity of analyzed problem is connected with the

fact that in moderate Reynolds number flow the effects of inertia, pressure and viscous forces are all significant and have to be taken into account [Panton 2005]. What is more the problem grows complicated as we bear in mind that there is no sudden change in flow pattern between low Reynolds number flow, where viscous effects are dominating into moderate Reynolds number.
The effects described here depend explicitly on Reynolds number, which means that velocity can change the flow pattern drastically by changing the dominating effect. That gives us a novel, precise tool of controlling the streak cross-section shape and its wall contact area which can be used in hydrodynamic focusing applications.

Acknowledgments

The authors wish to thank the Ministry of Science and Higher Education of Poland for financial support within project No. N N208 2943 33

References

Dziubinski M., Domagalski P.M., (2007), *Chemical and Process Engineering*, in press.

Kam L., Boxer S.G., (2003), *Langmuir*, 19, 1624-1631.

Kamholz A.E., Yager P., (2001), *Biophysical Journal*, 80(1), 155-160.

Kenis P.J.A., Iismagilov R.F., Whitesides G.M., (1999), *Science*, 285(5424), 83-85.

Lunde I., (2005), *M.Sc. Pre-project, Dept. Of Energy and Process Engineering, NTNU*.

Mielnik M.M., Ekatpure R.P., Sætran L.R., Schönfeld F., (2005), *Lab Chip*, 5, 897–903.

Moffatt H.K, (1964), *J. Fluid Mech*. 18, 1-18.

Park J.S., Choi C.K., Kihm K.D., (2004), *Exp fluids* 37, 105–119.

Reynolds O., (1883), *Phil. Trans. R. Soc*. 174, 935-982.

Ronald L. Panton, *Incompressible Flow*, Wiley (2005)

Takayama S., Ostuni E., Leduc P., Naruse K., Ingber D.E., Whitesides G.M., (2003), *Chemistry & Biology*, 10,123-130.